

See discussions, stats, and author profiles for this publication at: <https://www.researchgate.net/publication/256449205>

Evolutionary Origins of the Photosynthetic Water Oxidation Cluster: Bicarbonate Permits Mn²⁺ Photo-oxidation by Anoxygenic Bacterial Reaction Centers

ARTICLE *in* CHEMBIOCHEM · SEPTEMBER 2013

Impact Factor: 3.09 · DOI: 10.1002/cbic.201300355 · Source: PubMed

CITATION

1

READS

51

6 AUTHORS, INCLUDING:



Andrei A Khorobrykh

Russian Academy of Sciences

16 PUBLICATIONS 83 CITATIONS

SEE PROFILE



Derrick R J Kolling

Marshall University

29 PUBLICATIONS 743 CITATIONS

SEE PROFILE



Vyacheslav Klimov

Russian Academy of Sciences

179 PUBLICATIONS 4,262 CITATIONS

SEE PROFILE



Gerard Charles Dismukes

Rutgers, The State University of New Jersey

223 PUBLICATIONS 9,082 CITATIONS

SEE PROFILE

Evolutionary Origins of the Photosynthetic Water Oxidation Cluster: Bicarbonate Permits Mn^{2+} Photo-oxidation by Anoxygenic Bacterial Reaction Centers

Andrei Khorobrykh,^[a] Jyotishman Dasgupta,^[b] Derrick R. J. Kolling,^[b] Vasily Terentyev,^[a] Vyacheslav V. Klimov,^{*[a]} and G. Charles Dismukes^{*[c]}

In memory of Ivano Bertini

The enzyme that catalyzes water oxidation in oxygenic photosynthesis contains an inorganic cluster (Mn_4CaO_5) that is universally conserved in all photosystem II (PSII) protein complexes. Its hypothesized precursor is an anoxygenic photobacterium containing a type 2 reaction center as photo-oxidant (bRC2, iron–quinone type). Here we provide the first experimental evidence that a native bRC2 complex can catalyze the photo-oxidation of Mn^{2+} to Mn^{3+} , but only in the presence of bicarbonate concentrations that allows the formation of $(\text{bRC2})\text{Mn}^{2+}(\text{bicarbonate})_{1-2}$ complexes. Parallel-mode EPR spectroscopy was used to characterize the photoproduct,

$(\text{bRC2})\text{Mn}^{3+}(\text{CO}_3^{2-})$, based on the g tensor and ^{55}Mn hyperfine splitting. (Bi)carbonate coordination extends the lifetime of the Mn^{3+} photoproduct by slowing charge recombination. Prior electrochemical measurements show that carbonate complexation thermodynamically stabilizes the Mn^{3+} product by 0.9–1 V relative to water ligands. A model for the origin of the water oxidation catalyst is presented that proposes chemically feasible steps in the evolution of oxygenic PSII, and is supported by literature results on the photoassembly of contemporary PSII.

Introduction

Oxygenic photosynthesis is widely accepted as the dominant source of atmospheric oxygen. It is believed to have emerged very early in earth's history, approximately 2.2 to 2.8 bya (or even earlier), based on various indirect geochemical and fossil lines of evidence.^[1] This biological innovation was a seminal event in evolution as it enabled water to serve as an electron donor, thus allowing oxygenic photosynthesis to occur everywhere on earth's vast water system. This oxygenic transition permitted the subsequent evolution of energy-efficient respiratory metabolisms that power all oxygen-dependent life on earth.^[1] How the former bio-geochemical innovation occurred is the subject of wide interest and scientific debate. The question has been considered from several perspectives,^[2] from the organismal precursor—a presumed anoxygenic photosynthetic

bacterium lacking an oxygenic photoreaction center protein complex that converts visible light energy by single-electron/hole charge separation steps—to the nature of the inorganic catalyst that captures the RC-generated holes, and finally to the generation of molecular oxygen (O_2) and free protons. Contrary to simplistic (nonchemical) models for the latter process, the catalyst is not merely a site that stores four electron vacancies and releases protons at the correct redox potential.


All contemporary oxygenic phototrophs contain two types of reaction centers, denoted RC1 (iron–sulfur) and RC2 (iron–quinone).^[3] Water oxidation in all oxygenic phototrophs is driven photochemically by an oxygenic RC2 called photosystem II (PSII) and its associated inorganic water oxidation complex (PSII–WOC). Models for its origin have been proposed based on different criteria, from the chemistry of the water oxidation reaction,^[4] to the sequence and structure of the PSII subunits,^[5] as well as more widely essential bacterial genetic marker such as 16S rRNA phylogeny (protein biosynthesis).^[6] Based on sequence and cofactor similarity, it has been generally accepted that the four core chlorophyll-binding subunits of PSII (D1, D2, CP43, and CP47) are the result of the acquisition and evolution of two copies of an ancestral RC1 gene that split into an antenna domain (N-terminal domain of *psaA*) and a reaction center domain (the L (*pufL*) and M (*pufM*) RC2 subunits).^[5b,7] D1 is functionally equivalent to L (binding to the second quinone acceptor Q_B), and D2 is functionally equivalent to M (binding to the primary quinone acceptor Q_A).^[5b,8] whereas CP43 (*psbC*) and CP47 (*psbB*) are functionally equivalent to

[a] Dr. A. Khorobrykh,⁺ Dr. V. Terentyev, Prof. Dr. V. V. Klimov
Institute of Basic Biological Problems, Russian Academy of Sciences
Pushchino, 142290 (Russia)
E-mail: vklimov@rambler.ru

[b] J. Dasgupta,⁺ Dr. D. R. J. Kolling
Frick Laboratory, Department of Chemistry, Princeton University
Princeton, NJ 08544 (USA)

[c] Prof. Dr. G. C. Dismukes
Department of Chemistry & Chemical Biology and
the Waksman Institute of Microbiology, Rutgers University
610 Taylor Road, Piscataway, NJ 08854 (USA)
E-mail: dismukes@rci.rutgers.edu

[⁺] These authors contributed equally to this work.

 Supporting information for this article is available on the WWW under
<http://dx.doi.org/10.1002/cbic.201300355>.

the N-terminal domain of homodimeric RC1 *psaA*.^[5b,7a] The proposed evolutionary lineage of PSII from bacterial RC2 (bRC2) is also supported by gene synteny. The genome of cyanobacterium *Gloeobacter violaceus*, the earliest branching cyanobacterium in the tree of life, encodes an operon of three cotranscribed PSII RC genes, *psbADC*, that parallels the organization of the *pufLM* operon for bRC2 that is universally cotranscribed in all anoxygenic type 2 bacteria.^[9] By contrast, the *psbA* gene locus within the genomes of all more recently evolved oxygenic phototrophs, including other cyanobacteria, eukaryotic algae and plants, is well separated from all other PSII subunits.

The inorganic core that catalyzes water oxidation in all contemporary PSII-WOCs is highly conserved across all oxygenic phototrophs.^[10] There are no natural variations with different inorganic cofactors than the canonical Mn_4CaO_5 WOC. The inorganic core is not isolable as it is unstable free of PSII and must be assembled one atom at a time within apo-WOC-PSII by the photo-oxidation of four Mn^{2+} in the presence of Ca^{2+} , HCO_3^- , Cl^- and an electron acceptor. The first step involves the photo-oxidation of Mn^{2+} to Mn^{3+} coordinated to bicarbonate and apo-WOC-PSII.^[11] Electrochemical studies have shown that (b)carbonate complexation to Mn^{2+} reduces the standard oxidation potential from 1.51 at pH 0 for $\text{Mn}^{2+}_{\text{aq}}$ (1.18 V at pH 7) to 0.52–0.68 V (at pH 5.5–8.5) by stabilizing Mn^{3+} , forming adducts with one to three (b)carbonate ligands.^[12] Coincidentally, this potential is equal to the midpoint potential of the primary electron donor in bRC2s. Other studies have shown that exogenous Mn^{2+} with added bicarbonate enabled electron donation to bRC2s from *Rhodobacter sphaeroides* that were genetically engineered to produce a more oxidizing photooxidant (P^+/P) electrochemical potential (shifts by +0.25 V) and a carboxylate binding site for binding Mn^{2+} .^[13] Until now, native bRC2s have not been known to be able to oxidize Mn^{2+} . In this report, we show that the addition of bicarbonate specifically enables photo-oxidation of Mn^{2+} by bRC2 from the purple anoxygenic bacterium *Rhodovulum iodolum*. Using parallel- and perpendicular-mode EPR spectroscopy we show that this process involves the formation of a ternary complex, $\text{Mn}^{3+}(\text{HCO}_3)_x\text{bRC2}$. Together with published data this information is used to build a more detailed model for the evolutionary steps that might have led to an oxygenic RC precursor.

Results

Figure 1 shows the characteristic six-line EPR signal of aqueous Mn^{2+} (d^5 , $S=5/2$) arising from the isotropic hyperfine coupling with ^{55}Mn nucleus ($I=5/2$).^[12] Upon illumination at room temperature (880 nm LED, intensity 32 mW cm^{-2}) for 3 min the Mn^{2+} signal intensity decreases (ca. –5%), while a narrow $g=2.0$ radical signal appears that is due to the formation of the P870^+ radical cation. In the absence of added Mn^{2+} , the yield of the radical EPR signal is larger by the same amount; this is consistent with our previous report based on UV–visible absorbance change.^[15] To follow the temporal dependence of the change in Mn^{2+} concentration and to avoid the influence of intensity changes from the radical signal, the EPR signal intensity was measured at 3201 G, which corresponds to the peak

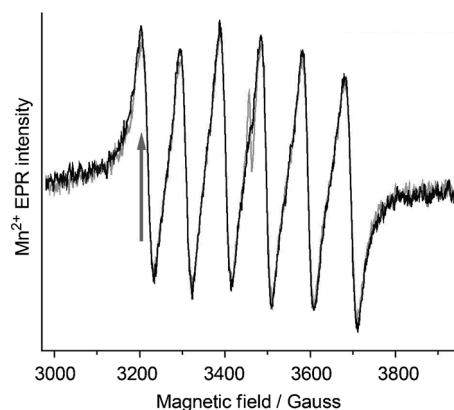


Figure 1. Mn^{2+} (250 μM) EPR measurements in the presence of bRC (3 μM) at 295 K. The initial trace, following 15 min dark incubation, is shown in black. After illumination at 880 nm for 3 min, the Mn^{2+} signal intensity decreases (–5%, approximately; gray trace); this is accompanied by an increase in the radical signal at $g=2.00$, which corresponds to the P^+ radical of bRC. EPR parameters: microwave frequency = 9.70 GHz, microwave power = 20 dB. Details of the sample are specified in the text.

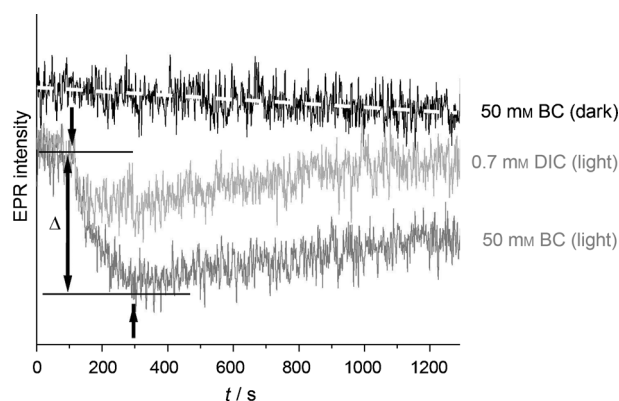


Figure 2. Mn^{2+} EPR signal intensity at its peak (3201 G) upon 880 nm illumination of bRC at room temperature. Bottom trace: with added NaHCO_3 (50 mM, pH 8.3); middle trace: with atmospheric dissolved inorganic carbon (total DIC = 0.7 mM, in 20 mM Tris, pH 8.3). The illumination period (3 min) is marked by Δ . The top trace shows the baseline of Mn^{2+} in 50 mM NaHCO_3 in the dark; the dashed line superimposed on the black trace shows the average rate of precipitation of MnCO_3 in the dark. BC = bicarbonate.

of the lowest-field ^{55}Mn hyperfine transition (Figure 2). As blank controls, we used Mn^{2+} samples with or without added bicarbonate. In the absence of added bicarbonate, the Mn^{2+} signal was indefinitely kinetically stable in the dark. In the presence of 50 mM bicarbonate, the Mn^{2+} EPR intensity decreased slowly in the dark ($t_{1/2} \sim 60$ min) due to the precipitation of solid MnCO_3 which is not EPR active under these conditions (Figure 2, black trace).^[13] The bRC protein concentrations that we used (3–20 μM) did not influence the kinetics of this dark (background) chemistry as it was at a concentration 100 times lower than Mn^{2+} . Illumination at 880 nm of a sample containing bRCs (3 μM) in the presence of Mn^{2+} (250 μM) and dissolved inorganic carbon from atmospheric CO_2 (DIC = 0.7 mM in 20 mM Tris, pH 8.3) decreased the Mn^{2+} EPR signal (Figure 2, middle trace). Without illumination, this sample exhibited the same baseline as the control (black trace). After the light was

switched off (3 min), the Mn^{2+} signal recovered fully to the original baseline in approximately 5 min. Upon the addition of sodium bicarbonate, the yield of the photobleached Mn^{2+} increased up to threefold (at 50 mM sodium bicarbonate) with no change in the initial rate of signal bleaching (Figure 2, bottom trace); subsequent recovery in the dark had an appreciably longer half-life of approximately 15 min. The yield of the photobleached signal saturated as the bicarbonate concentration increased to 50 mM, but there was also greater interference from the more rapid precipitation of MnCO_3 in the dark and this prevented use of higher concentrations.^[15]

These results are consistent with our previous UV–visible electronic absorption spectroscopy measurements, which showed that the addition of Mn^{2+} in the presence of bicarbonate reduced the yield of photoinduced P^+ and accelerated its re-reduction in the dark.^[15,18] Additionally, it was shown that substituting Mn^{2+} with either Mg^{2+} or bicarbonate with formate increased the yield of photoinduced P^+ to the same as that observed without Mn^{2+} and bicarbonate. This result was taken as evidence that bicarbonate and Mn^{2+} are both essential for loss of the P^+ signal.

In order to determine if this lower photoinduced P^+ signal is due to chemical reduction of P^+ by $[\text{Mn}(\text{HCO}_3)_n]^{(2-n)+}$, EPR measurements were carried out at 5 K to detect possible oxidized photoproducts. No new signals were detected when using conventional (perpendicular) mode EPR in the range 0 to 4000 G, thereby excluding the formation of Mn^{4+} or spin-coupled Mn dimers (not shown). Parallel-mode microwave excitation was used to characterize the anticipated Mn^{3+} complex. Figure 3 shows the parallel-polarization EPR difference spectrum of the bRC sample in 50 mM sodium bicarbonate, obtained after 5 min of illumination at 880 nm followed by quench cooling in dry ice/methanol. Apart from cooling, these are the same conditions as those that bleach the room-temperature Mn^{2+} EPR signal reported in Figure 2 (raw data are given in Figure S1 in the Supporting Information). A six-line

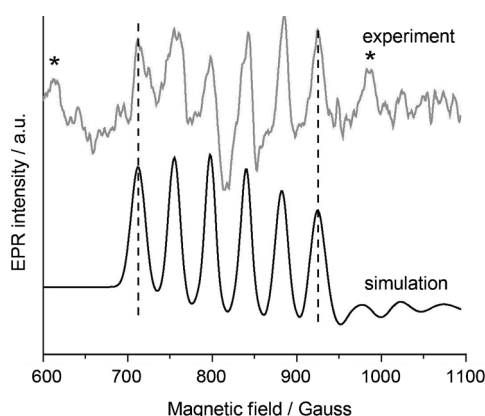


Figure 3. Top: parallel-mode EPR signal of photogenerated Mn^{3+} from the bRC sample in Figure 2 (Light minus dark difference spectrum). Sample was illuminated for 5 min at 273 K and quench cooled in dry ice/methanol. The medium contained 20 mM Tris-HCl, 500 μM MnCl_2 , 20 μM bRC, 50 mM NaHCO_3 (pH 8.3). EPR parameters: microwave frequency = 9.324 GHz; microwave power = 50 mW. Bottom: a spectrum simulated by using the spin Hamiltonian parameters described in the text.

EPR spectrum forms at $g_{\text{eff}} \sim 8$ upon illumination. This signal is assigned to a Mn^{3+} ion in a rhombically distorted ligand field based on its g value and the six-line splitting indicative of ^{55}Mn hyperfine splittings.^[19] In contrast, no stable Mn^{3+} EPR signal was produced by illumination in the absence of added sodium bicarbonate (20 mM Tris buffer, pH 8.3, DIC = 0.7 mM; Figure S1). A simulation of the Mn^{3+} signal^[16] was performed by taking into account both rhombic zero-field splitting of the $S = 2$ ground state (ZFS, $E/D > 0$) and ^{55}Mn hyperfine tensors (see the Supporting Information). The center of the six-line pattern occurs at $g_{\text{eff}} = 8.133$, and the hyperfine splitting is $A_{\text{ZZ}} = 42$ G.

The yield of the photogenerated Mn^{3+} was conservatively estimated to be approximately 4 μM , based on comparison to a Mn^{3+} spin standard: Mn^{3+} -meso-tetrakis(*N,N*-dimethyl-imidazo-2-yl)porphyrin (TDMImP; Figure S2). This estimate assumes that the intrinsic transition probability of the standard is the same as that of the new signal, which is equivalent to assuming they have the same ratio of rhombic to axial ligand field terms (E/D).^[19b,c] This yield is approximately 20% of the initial bRC content of the sample. From this accumulated yield and the time of illumination (5 min) the actual quantum yield must be considerably lower, below 0.1 %

In the absence of added bicarbonate but the presence of DIC ([DIC]_{total} = 0.7 mM at 20 mM Tris, pH 8.3), we observed a lower level of continuous bRC-mediated photobleaching of Mn^{2+} at room temperature and no visible EPR signal for Mn^{3+} (data not shown). We attribute this photobleaching to the same photo-oxidation process, but at lower conversion due to the much lower bicarbonate level. Because the dissociation constant for aqueous $\text{Mn}^{2+}(\text{CO}_3^{2-})$ is considerably higher (ca. 50 mM) than the concentrations used,^[12] only a minor fraction of the Mn^{2+} was present as the (b)carbonato form. The Mn^{2+} photobleaching rate slowed as the bicarbonate concentration decreased.

Discussion

The $g_{\text{eff}} = 8.133$ and ^{55}Mn hyperfine splitting ($A_{\text{ZZ}} = 42$ G) of the Mn^{3+} (b)carbonato photoproduct from bRC are similar to the values observed for the Mn^{3+} (b)carbonato–PSII ternary complex in spinach formed by photo-oxidation of Mn^{2+} at the high-affinity site in apo-WOC–PSII during the first step of photoassembly from the free inorganic cofactors (formation of IM1).^[19a,b] Our prior analysis has shown that for these values of g_{eff} and A_{ZZ} , the ground state of Mn^{3+} corresponds to $^5\text{B}_{1g}$, in which the $3d^4$ valence electronic configuration has the hole mainly in the $d_{x^2-y^2}$ orbital. This is the common situation for the tetragonal ligand fields typical of six-coordination geometry and contrasts with $^5\text{A}_{1g}$, which has the hole in the d_{z^2} orbital and for which $A_{\text{ZZ}} \sim 100$ G. The latter situation occurs more commonly in five-coordinate trigonal bipyramidal ligand fields.

The parallel-mode EPR spectral parameters of Mn^{3+} in IM1 formed during PSII photoassembly (g value, ^{55}Mn hyperfine coupling constant (A_z) and the ligand-field splitting parameters, D/E) were previously shown to depend on the interaction of bicarbonate with Mn^{3+} . In particular, all three parameters became independent of solution pH (6 to 9.5), in marked con-

trast to their strong pH dependence in the absence of bicarbonate. (Bi)carbonate coordination “chemically isolates” the Mn^{3+} in IM1 from external pH changes, and directly influences the ligand-field strength and its symmetry. The Mn^{3+} IM1 site has been identified as the *exo*-cuboidal Mn atom (Mn #4) in the X-ray diffraction atomic structure of PSII, based on EPR analysis of ligand hyperfine coupling^[19a] and photoassembly kinetics.^[10,11b]

The formation of IM1 is followed by the rate-limiting dark step of photoassembly, which involves the binding of Ca^{2+} coupled to a protein conformational change thought to involve the carboxyl terminal domain of the D1 subunit of PSII. This generates an oxo-bridged binuclear unit, $[\text{Mn}-\text{O}-\text{Ca}]^{3+}$, that is bound to the D1 folded carboxyl domain. This folded structure provides the sites for binding the remaining three Mn^{2+} and photo-oxidation to form the heterocubane core, $[\text{Mn}_3\text{CaO}_4]^{n+}$. We believe that bicarbonate-enabled formation of IM1 and folding of the D1 carboxyl terminus could have played crucial roles in the evolution of the WOC of PSII, as described next.

Postulated model for the evolution of the oxygenic reaction center

It has been estimated that during the Archean geological era, the atmospheric CO_2 partial pressure was 30 to 3000 times

greater than contemporary levels.^[4b] Under such conditions, the chemical speciation of aqueous Mn^{2+} would have been dominated by 1:1 and 1:2 $\text{Mn}:(\text{bi})\text{carbonato}$ complexes at neutral pH.^[12,20] The standard electrochemical reduction potentials for the corresponding $\text{Mn}^{3+}/\text{Mn}^{2+}$ redox couples of these species shift appreciably to $E^0 = 0.52\text{--}0.68\text{ V}$ at pH 8.3 from the aquo- $\text{Mn}^{3+}/\text{Mn}^{2+}$ value of $E^0 = 1.51\text{ V}$.^[12,20,21] This large 1 V shift arises from stabilization of the Mn^{3+} carbonato product and is significantly larger than that observed with carboxylato complexes (acetate, formate, oxalate). One outcome of this stabilization is that $\text{Mn}^{2+}(\text{bi})\text{carbonato}$ complexes are thermodynamically feasible electron donors to P^+ in bRCs.

We previously used this energy concept to postulate a model for how bicarbonate complexation chemistry could have allowed anoxygenic phototrophs to utilize $\text{Mn}^{2+}(\text{bi})\text{carbonato}$ species as alternative electron donors to replace reduced carbon sources, thereby enabling the spread of early anoxygenic phototrophs to manganese-enriched ecological zones and providing the first step in the transition from anoxygenic to oxygenic photosynthesis.^[4b,9,22] A further elaboration of this model that postulates associated gene and protein evolution steps is given in Figure 4.

Our evolutionary model starts with a bRC2-containing anoxygenic phototroph as the immediate photosynthetic precursor. This bRC2 has a low quantum yield for the photo-oxidation of $\text{Mn}^{2+}(\text{bi})\text{carbonato}$ perhaps owing to the absence of a bind-

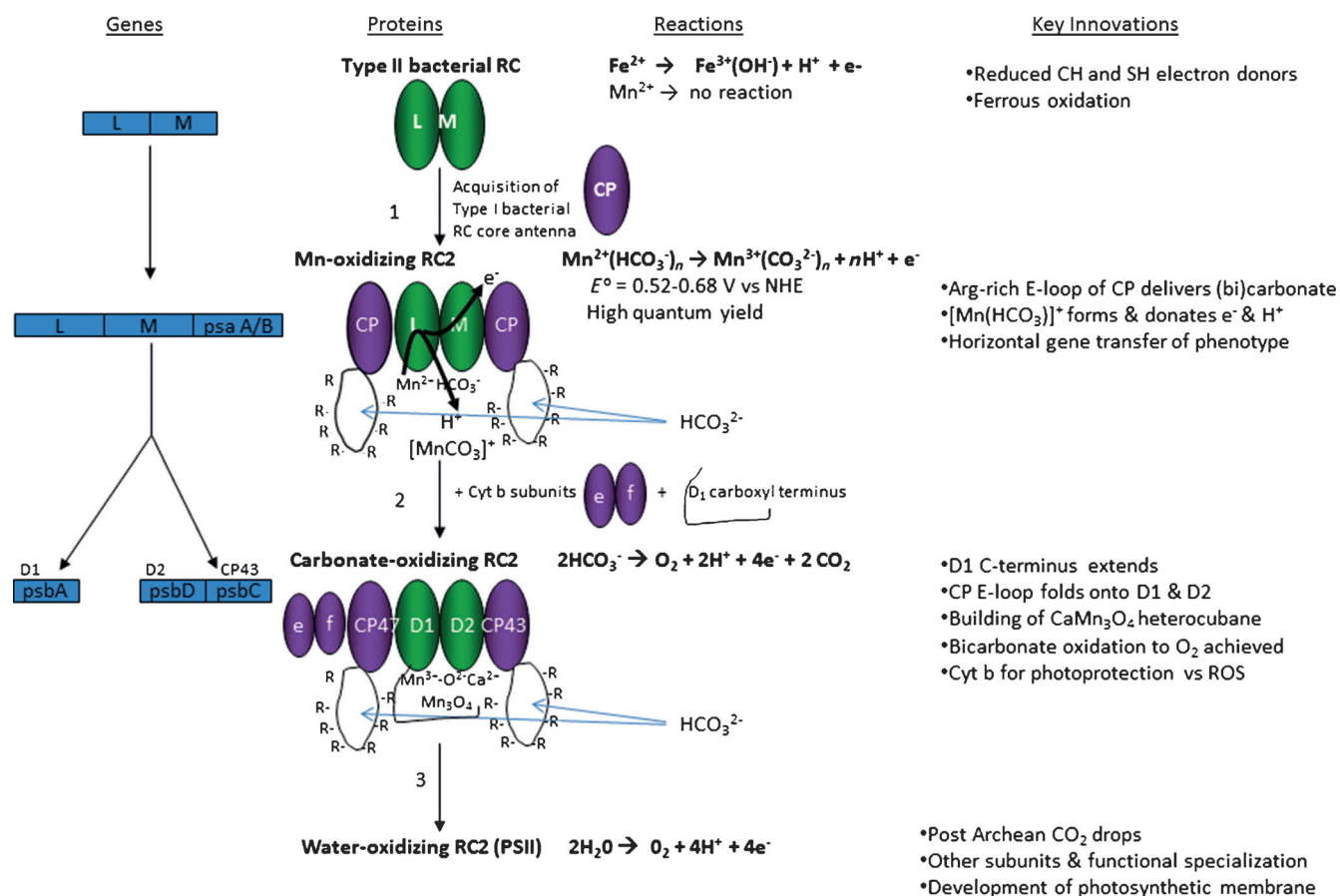


Figure 4. Postulated model for the chemically feasible steps in the evolution of the water oxidation complex of oxygenic photosystem II from the type 2 bacterial reaction center.

ing site and the limited availability of intracellular bicarbonate to allow speciation as Mn^{2+} (b)carbonate complexes. Contemporary cells contain multiple DIC-concentrating mechanisms that elevate intracellular concentrations of DIC to a level that can complex to Mn^{2+} . A cyanobacterial example is the hyper-carbonate-requiring *Arthrospira maxima*, which takes up high levels of DIC intracellularly specifically for the proton evolution activity of PSII (but not for electron donation to WOC).^[23] Multiple DIC-concentrating mechanisms exist in bacteria that evolved in response to the waning levels of CO_2 in the post-Archean era.^[4b,22] One such mechanism that is intrinsic to the PSII reaction center protein core could have been critical for the evolution of oxygenic RCs and is depicted in Figure 4.

The first step in our proposed evolutionary sequence is the acquisition of an intrinsic bicarbonate-buffering function within the reaction center that enabled cells to concentrate bicarbonate internally to sufficient levels that speciation of Mn^{2+} exists as Mn^{2+} (b)carbonate (step 1, Figure 4). For simplicity not all independent steps are shown. This chemistry allowed solar energy to drive electron and proton release from Mn^{2+} (b)carbonate to the RC and internal space. This $\text{Mn}^{3+}(\text{CO}_3^{2-})_n$ product forms at a specific (proximal) site and has several possible fates depending on the environment, including forming Mn oxide/carbonate oligomers, precipitating as colloidal Mn_2O_3 (an excellent water oxidation catalyst),^[24] or disproportionating to form colloidal MnO_2 (inactive catalytically). Evolution of a specific binding site for the Mn^{3+} product is a required part of this sequence and is postulated to result in the formation of manganese oxide oligomers, starting with the simple dimeric intermediate: $[\text{Mn}^{3+}(\text{O}^{2-})_2\text{Mn}^{2+}]^+$, in which carbonate serves as the oxide donor. To increase the carbonate concentration inside cells, there must be a carbonate-concentrating mechanism, such as that proposed next.

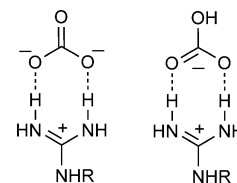
All PSII RCs have two subunits, denoted CP43 and CP47, that bind chlorophyll and serve as core antennas for light harvesting.^[25] These membrane-spanning subunits, especially CP47, have been proposed to originate from gene duplication of the six N-terminal transmembrane helical domains of the PsaA/PsaB reaction center proteins of photosystem I, denoted CP in Figure 4.^[25] Both CP47 and CP43 have an unusually long inter-helical loop between the two transmembrane helices at the carboxyl terminus (E loop, approximately 185 residues). The E loop is fully exposed to the aqueous domain at the luminal surface of the photosynthetic membrane and packs against the D1 (D2) luminal surface in the case of CP43 (CP47), close to where the WOC inorganic complex resides. A conserved arginine residue (CP47-R357) is found within the active site of all PSII-WOCs and functionally interacts with (b)carbonate during oxygen evolution activity of the intact holoenzyme.^[26] (B)carbonate enhances the rate of water oxidation in some PSII and protects against photoinhibition during extended illumination.^[27] The E loop of both CP subunits contains an unusually large number of arginine and lysine residues in all prokaryotic and eukaryotic PSII. For example, the 1.9 Å X-ray structure of *Thermosynechococcus vulcanus* PSII reveals seven Arg and four Lys (CP43) and twelve Arg and ten Lys (CP47).^[25a] The Arg side-chain residues contain the guanidinium cation, $\text{RHNC}(\text{NH}_2)=$

NH_2^+ , whereas Lys contains the amine cation RNH_3^+ ($\text{pK}_a=13.9$ and 10.1 , respectively). Some of these side chains are involved in salt bridges to anionic protein residues, others are implicated in binding free (nonprotein) anions. Notably, chloride and (b)carbonate are found within the luminal aqueous space and are needed for O_2 evolution activity.

The guanidinium cation is an especially good chelator of HCO_3^- and CO_3^{2-} , as well as of phosphate mono- and diesters (ROPO_3^{2-} , $(\text{RO})_2\text{PO}_2^-$), owing to the combination of bidentate H-bonding and ion-pairing interactions. Arginine/carbonate ion pairs are frequently found in the crystal structures of proteins.^[28] The free energy of guanidinium–carbonate ion pair formation is -4 kJ mol^{-1} for (b)carbonate in water, and estimated to be -16 kJ mol^{-1} (DMSO/water 80:20) for carbonate and structurally related dianions like phosphate monoesters.^[29] This range corresponds to formation constants of 4 to 500 M^{-1} , and this affinity enables Arg to take up (b)carbonate (and thus CO_2) from solution into cells. This combination of bidentate H-bonding and ion pairing significantly accelerates the rate of hydrolysis of carbonate esters and phosphate esters due to stabilization of the transition state (of the order of -12 kJ mol^{-1} [29a]). An important feature of (b)carbonate–guanidinium ion pairing is the distinctively increased molar conductivity at high dilutions.^[30] This feature is attributed to the basicity of the carbonate ion and the accompanying greater formation of OH^- and HCO_3^- relative to spontaneous water dissociation. The high mobility of the hydroxide ion in water leads to a significant increase in conductance. Because of the aforementioned lower energy barrier to hydrolysis in the (b)carbonate–guanidinium ion pair, rapid transport of added protons (i.e., generated by water oxidation) to regions of low concentration can be achieved.

By extension, these considerations suggest that the large number of highly conserved arginines in the E loop of CP proteins found among all oxygenic PSII serves a specific purpose in concentrating intracellular (b)carbonate within the aqueous luminal space and serving as a proton buffer to accelerate the water oxidation rate at high turnover rates (high light intensities). This luminal (b)carbonate buffer has been shown to serve two essential roles in some contemporary PSII: 1) it is indispensable for assembly of the Mn_4CaO_5 cluster during biogenesis and repair,^[11a,31] and 2) in some species of cyanobacteria (*Arthrospira maxima*) it plays an essential role in removing the substrate water protons formed during catalytic turnover.^[23]

The next major step in our proposed evolutionary sequence (step 2, Figure 4) would be the innovation of concerted four-electron oxidation function by the formation of a WOC inorganic core, $[\text{CaMn}_4\text{O}_5]$. We postulate that this manganese–calcium–oxide cluster was built in two stages and, based on thermodynamic preference, initially preferred bicarbonate over water as the substrate for oxidation.^[4b] first, by a chemical mechanism that restricts the number of oxidizable Mn^{2+} to



four (here proposed to be Ca^{2+} -dependent); second, by evolution of a protein binding domain that favors formation of the essential CaMn_3O_4 “heterocubane” subcluster (here proposed as the evolution of the D1 carboxyl extension). A hint at how this first condition might have occurred is taken from the slow dark step of photoassembly of contemporary apo-WOC-PSIIs, in which calcium binds and restricts the number of photo-oxidizable Mn^{2+} from 20 in its absence, to only four in its presence.^[32] During photoassembly, Ca^{2+} binds in the dark following photo-oxidation of the first Mn^{2+} (proximal or high-affinity site) and forms an oxido- (or bis-hydroxo-) bridged intermediate, $[\text{Mn}^{3+}(\text{O}^{2-})\text{Ca}^{2+}]^{3+}$.^[19b,c] Ca^{2+} affinity for the oxido/hydroxido anion is greater than that of Mn^{2+} , and this suppresses binding of the second Mn^{2+} at this site, thus eliminating hole transfer to it and further polymerization of manganese oxide. Strong vibronic coupling of the proximal Mn^{3+} to the oxide (Jahn–Teller effect) should localize the hole to the axial d_{z^2} orbital to form $\text{Mn}^{3+}(\text{O}^{2-})$, until the observed slow protein conformational change in the D1 subunit forms the higher-affinity binding site for the remaining three Mn^{2+} ions (and possibly bicarbonate).^[11b] Hole transfer to these distal Mn^{2+} (bicarbonate) ions would then become allowed upon delivery of a second oxide or hydroxide (from bicarbonate) to form $[\text{Mn}^{3+}(\text{O}^{2-})_2\text{Ca}^{2+}]^+$ and release a molecule of CO_2 . This nonaxial ligand field causes rehybridization of the proximal hole from the axial d_{z^2} orbital to populate one of the cloverleaf-type d orbitals directed at the two oxides (d_{xy}), thus forming a typical Mn^{3+} d^4 electron configuration and Jahn–Teller distorted ligand field. Coordination of three Mn^{2+} (bicarbonate) to these bridging oxides would then allow inner-sphere electron transfer of the proximal hole to these distal Mn^{2+} sites. Subsequent photo-oxidation of the reduced proximal Mn^{2+} site can then continue to deliver holes to the distal three Mn^{3+} to form the CaMn_3O_4 heterocubane subcluster.^[10] We postulate that bicarbonate was the preferred substrate for oxidation by this WOC precursor, given its high abundance in the CO_2 -rich environment of the Archean era and lower energy for oxidation versus water.^[4b] However, no evidence for carbonate oxidation by contemporary PSII–WOCs has yet been reported.

This postulated sequence of evolutionary innovations provides a unique role for Ca^{2+} in the evolution of the inorganic core that could contribute to its retention during the subsequent diversification of oxygenic phototrophs in step 3 of Figure 4. This diversification and the decrease in environmental CO_2 would ultimately result in the replacement of bicarbonate by water as substrate, perhaps driven by the greater proton yield and higher pmf (4H^+ instead of 2H^+). But no replacement for bicarbonate ion function in the photoassembly of the WOC appears to have been found, at least not one as rapid or as high yielding. O_2 evolution by water oxidation in these early oxygenic phototrophs would have been even more inefficient than today and probably even more compromised by the reduction of O_2 to superoxide, hydrogen peroxide, and hydroxyl radicals owing to the more reducing conditions of the Archean era. Mechanisms to suppress these damaging intermediates would likely have evolved early on. This theory forms the basis for our inclusion of a cytochrome *b* precursor to cyt-b559 in

the earliest oxygenic phototroph to serve in photoprotection, both as a superoxide dismutase^[33] and as required cofactor for cyclic electron transfer around PSII (step 2, Figure 4).

Experimental Section

Rhodovulum iodosum sp. is a marine phototrophic purple bacterium that is capable of oxidizing extracellular ferrous iron.^[14] In terms of its photosynthetic apparatus it is, however, organized analogously to more commonly studied purple bacteria (e.g., *R. sphaeroides*) based on previous P870+ optical spectroscopy experiments. We isolated bacterial reaction center complexes (RC-LH1) from *R. iodosum* as previously described.^[15] Buffer exchange was performed with Tris-HCl (20 mM), NaCl (25 mM) and dodecyl maltoside (0.03%, w/v) to carry out measurements at pH 8.3. For room-temperature EPR measurements, MnCl_2 (250 or 500 μM) and NaHCO_3 (50 mM, pH 8.3) were added in the dark to bRC (3 μM). The EPR signals of aqueous solutions were measured by using a quartz flat cell in a standard TM102 cavity at a microwave (MW) frequency of 9.70 GHz. Transient EPR spectra of photo-oxidized Mn^{2+} bRC2 solutions were recorded both in the dark and under 880 nm LED illumination at room temperature (intensity 32 mW cm^{-2}). Mn^{3+} EPR signals were measured on a Bruker Elexsys 580 X-band spectrometer with Bruker ER 9601 DM dual-mode cavity and Oxford ESR 900 helium-flow cryostat (Oxford Inst). For these measurements, samples of identical volumes were placed in precision quartz tubes both in the presence and absence of added bicarbonate prior to being frozen in a dry-ice bath, followed by immersion in liquid nitrogen. For Mn^{3+} detection at 5 K, the Mn^{2+} -bound bRC samples (20 μM) were measured as prepared in the dark and also after illumination at 0 °C. The “dark-minus-light” difference spectrum corresponds to the photo-oxidizable Mn^{2+} that is bound to bRCs. EPR simulations were performed by using the MATLAB EasySpin package.^[16]

To determine the total dissolved inorganic carbon (DIC) concentration, we used a LICOR LI-6252 CO_2 analyzer. Tris buffer solutions at 50 and 20 mM contained 1.60 ± 0.02 and 0.7 mM DIC, respectively, upon equilibration with the atmosphere. The lower Tris concentration was used as it contained less DIC (its main purpose) yet retained good buffer capacity at the same pH (8.3) as the sodium bicarbonate buffer. Our results agree with a literature report that found that Tris-buffered solutions increase the DIC from atmospheric CO_2 at commonly used buffering concentrations.^[17]

Acknowledgements

This research was supported by grants from the NSF (CHE-1213772) to G.C.D., the Russian Foundation for Basic Research of the Academy of Sciences to V.V.K. and A.A.K., by a CRDF for travel fellowship, and fellowships from NASA-NAI to J.D. and the Dreyfus Foundation and the ACS to D.R.J.K. We thank John T. Groves for a sample of Mn^{3+} -TDMelMP and David Vinyard for editing the manuscript.

Keywords: bacterial reaction centers • bicarbonate • evolution • manganese • oxygenic photosynthesis • photosystem II

- [1] a) J. F. Allen, W. Martin, *Nature* **2007**, *445*, 610–612; b) J. F. Kasting, *Science* **1993**, *259*, 920–926.

- [2] J. Raymond, R. E. Blankenship, *Biochim. Biophys. Acta Bioenerg.* **2004**, 1655, 133–139; b) "The Origin and Evolution of Photosynthetic Oxygen Production", G. C. Dismukes, R. E. Blankenship in *Photosystem II: The Water/Plastoquinone Oxido-Reductase in Photosynthesis* (Eds.: T. Wydrzynski, K. Satoh), Springer, Dordrecht, **2005**; c) K. Fennel, M. Follows, P. G. Falkowski, *Am. J. Sci.* **2005**, 305, 526–545; d) M. L. Ginger, G. I. McFadden, P. A. M. Michels, *Philos. Trans. R. Soc. B* **2010**, 365, 693–698; e) T. Dagan, M. Roettger, K. Stucken, G. Landan, R. Koch, P. Major, S. B. Gould, V. V. Goremykin, R. Rippka, d. M. N. Tandeau, M. Gugger, P. J. Lockhart, J. F. Allen, I. Brune, I. Maus, A. Puehler, W. F. Martin, *Genome Biol. Evol.* **2013**, 5, 31–44.
- [3] J. F. Allen, *FEBS Lett.* **2005**, 579, 963–968.
- [4] a) R. E. Blankenship, H. Hartman, *Trends Biochem. Sci.* **1998**, 23, 94–97; b) G. C. Dismukes, V. V. Klimov, S. V. Baranov, Y. N. Kozlov, J. DasGupta, A. Tyryshkin, *Proc. Natl. Acad. Sci. USA* **2001**, 98, 2170–2175.
- [5] a) A. Y. Mulkidjanian, W. Junge, *Photosynth. Res.* **1997**, 51, 27–42; b) W.-D. Schubert, O. Klukas, W. Saenger, H.-T. Witt, P. Fromme, N. Krauß, *J. Mol. Biol.* **1998**, 280, 297–314; c) J. P. Allen, J. C. Williams, *Photosynth. Res.* **2011**, 107, 59–69.
- [6] G. J. Olsen, C. R. Woese, R. Overbeek, *J. Bacteriol.* **1994**, 176, 1–6.
- [7] a) F. Baymann, M. Brugna, U. Muhlenhoff, W. Nitschke, *Biochim. Biophys. Acta Bioenerg.* **2001**, 1507, 291–310; b) J. Raymond, R. E. Blankenship, *Biochim. Biophys. Acta Bioenerg.* **2004**, 1655, 133–139; c) J. F. Allen, W. F. Vermaas in *Encyclopedia of Life Sciences*, Wiley, Chichester, UK, **2010**.
- [8] a) H. Michel, J. Deisenhofer, *Biochemistry* **1988**, 27, 1–7; b) P. J. Lockhart, M. A. Steel, A. W. D. Larkum, *FEBS Lett.* **1996**, 385, 193–196.
- [9] T. A. Nguyen, J. Brescic, D. J. Vinyard, T. Chandrasekar, G. C. Dismukes, *Mol. Biol. Evol.* **2012**, 29, 35–38.
- [10] D. J. Vinyard, G. M. Ananyev, G. C. Dismukes, *Annu. Rev. Biochem.* **2013**, 82, 577–606.
- [11] a) S. Baranov, A. Tyryshkin, D. Katz, G. Dismukes, G. Ananyev, V. Klimov, *Biochemistry* **2004**, 43, 2070–2079; b) J. Dasgupta, G. M. Ananyev, G. C. Dismukes, *Coord. Chem. Rev.* **2008**, 252, 347–360.
- [12] J. Dasgupta, A. M. Tyryshkin, Y. N. Kozlov, V. V. Klimov, G. C. Dismukes, *J. Phys. Chem. B* **2006**, 110, 5099–5111.
- [13] a) L. Kálmán, R. LoBrutto, J. P. Allen, J. C. Williams, *Biochemistry* **2003**, 42, 11016–11022; b) M. Thielges, G. Uyeda, A. Cámara-Artigas, L. Kálmán, J. C. Williams, J. P. Allen, *Biochemistry* **2005**, 44, 7389–7394.
- [14] K. L. Straub, F. A. Rainey, F. Widdel, *Int. J. Syst. Bacteriol.* **1999**, 49, 729–735.
- [15] A. A. Khorobrykh, V. V. Terentyev, S. K. Zharmukhamedov, V. V. Klimov, *Philos. Trans. R. Soc. B* **2008**, 363, 1245–1251.
- [16] S. Stoll, A. J. Schweiger, *J. Magn. Reson.* **2006**, 178, 42–45.
- [17] R. G. Bates, H. B. Hetzer, *Anal. Chem.* **1961**, 33, 1285.
- [18] V. V. Terentyev, A. Y. Shkuropatov, V. A. Shkuropatova, V. A. Shuvalov, V. V. Klimov, *Biochemistry (Moscow)* **2011**, 76, 1360–1366.
- [19] a) K. A. Campbell, D. A. Force, P. J. Nixon, F. Dole, B. A. Diner, R. D. Britt, *J. Am. Chem. Soc.* **2000**, 122, 3754–3761; b) J. Dasgupta, A. M. Tyryshkin, S. V. Baranov, G. C. Dismukes, *Appl. Magn. Reson.* **2010**, 37, 137–150; c) A. M. Tyryshkin, R. K. Watt, S. V. Baranov, J. Dasgupta, M. P. Hendrich, G. C. Dismukes, *Biochemistry* **2006**, 45, 12876–12889.
- [20] Y. N. Kozlov, S. K. Zharmukhamedov, K. G. Tikhonov, J. Dasgupta, A. A. Kazakova, G. C. Dismukes, V. V. Klimov, *Phys. Chem. Chem. Phys.* **2004**, 6, 4905–4911.
- [21] *Encyclopedia of Electrochemistry of the Elements* (Eds.: C. Liang, A. J. Bard), Marcel Dekker, New York, **1973**, p. 351.
- [22] a) M. J. Russell, *Acta Biotheor.* **2007**, 55, 133–179; b) D. W. Schwartzman, C. H. Lineweaver, *Origins Life Evol. Biospheres* **2006**, 36, 205–206.
- [23] D. Carrieri, G. Ananyev, T. Brown, G. C. Dismukes, *J. Inorg. Biochem.* **2007**, 101, 1865–1874.
- [24] D. M. Robinson, Y. B. Go, M. Mui, G. Gardner, Z. Zhang, J. Li, M. Greenblatt, G. C. Dismukes, *J. Am. Chem. Soc.* **2013**, 135, 3494–3501.
- [25] a) T. Bricker, L. Frankel, *Photosynth. Res.* **2002**, 72, 131–146; b) J. Barber, E. Morris, C. Büchel, *Biochim. Biophys. Acta Bioenerg.* **2000**, 1459, 239–247.
- [26] G. M. Ananyev, T. Nguyen, C. Putnam-Evans, G. C. Dismukes, *Photochem. Photobiol. Sci.* **2005**, 4, 991–998.
- [27] V. V. Klimov, S. V. Baranov, *Biochim. Biophys. Acta Bioenerg.* **2001**, 1503, 187–196.
- [28] J. A. Ippolito, R. S. Alexander, D. W. Christianson, *J. Mol. Biol.* **1990**, 215, 457–471.
- [29] a) D. O. Corona-Martinez, O. Taran, A. K. Yatsimirsky, *Org. Biomol. Chem.* **2010**, 8, 873–880; b) P. E. Mason, G. W. Neilson, S. R. Kline, C. E. Dempsey, J. W. Brady, *J. Phys. Chem. B* **2006**, 110, 13477–13483.
- [30] J. Hunger, R. Neueder, R. Buchner, A. Apelblat, *J. Phys. Chem. B* **2013**, 117, 615–622.
- [31] S. V. Baranov, G. M. Ananyev, V. V. Klimov, G. C. Dismukes, *Biochemistry* **2000**, 39, 6060–6065.
- [32] a) G. M. Ananyev, L. Zaltsman, C. Vasko, G. C. Dismukes, *Biochim. Biophys. Acta Bioenerg.* **2001**, 1503, 52–68; b) G. M. Ananyev, A. Murphy, Y. Abe, G. C. Dismukes, *Biochemistry* **1999**, 38, 7200–7209; c) C. Chen, J. Kazimir, G. M. Cheniae, *Biochemistry* **1995**, 34, 13511–13526.
- [33] G. Ananyev, G. Renger, U. Wacker, V. Klimov, *Photosynth. Res.* **1994**, 41, 327–338.

Received: June 1, 2013

Published online on September 4, 2013